Exchange-Biasing in a Dinuclear Dysprosium(III) Single-Molecule Magnet with a Large Energy Barrier for Magnetization Reversal

Tian Han,[a] Marcus J. Giansiracusa,[b] Zi-Han Li,[a] You-Song Ding,[a],[b] Nicholas F. Chilton,[b] Richard E. P. Winpenny[b] and Yan-Zhen Zheng*[a]

Abstract: A dichlorido-bridged dinuclear dysprosium(III) single-molecule magnet $[Dy_2L_2(\mu\text{-}Cl)_2(THF)_2]$ has been made using a diamine-bis(phenolate) ligand, H_2L. Magnetic studies show an energy barrier for magnetization reversal (U_{eff}) around 1000 K. Exchange-biasing effect is clearly seen in magnetic hysteresis with steps up to 4 K. *Ab* initio calculations exclude the possibility of pure dipolar origin of this effect leading to the conclusion that super-exchange *via* the chloride bridging ligands is important.

Individual molecules that show slow relaxation of magnetisation are known as single-molecule magnets (SMMs).[1] This field started in 1993, and SMMs have been proposed as possible media for high-density magnetic storage.[2] A key parameter to evaluate the performance of an SMM is the effective energy barrier to magnetization reversal (U_{eff}). Dysprosium(III) is particularly preferred as the high magnetic anisotropy arising from the $^6H_{15/2}$ state generates the highest values for U_{eff} when placed in strong axial crystal fields. In particular, two Dy–SMMs families have very high U_{eff}: the sandwich structures with bis-cyclopentadienyl ligands[3] and pentagonal bipyramidal complexes.[4] In the latter, the strong axial crystal field is normally defined by short coordination bonds to the ligands on the axial positions of the pentagonal bipyramid.[4,5]

A feature common to many Dy–SMMs is loss of magnetization at zero field, which is attributed to the quantum tunneling of magnetization (QTM) under zero field.[3–6] Interactions between spin centers can prevent such zero-field loss of magnetization, known as exchange-bias. This was first seen[7] in a dimer of $[Mn_4]$ SMMs and has more recently been seen in Dy(III) dimers.[8] Our aim was to combine high U_{eff} values with exchange biasing by making a dimer of highly axial Dy(III) ions. For this strategy to work, the best molecular design would have the local anisotropy axes of the two Dy(III) sites as close as possible to being co-parallel.[9]

The title complexes $[RE_2L_2(\mu\text{-}Cl)_2(THF)_2]\cdot$toluene (RE = Dy, **1**; RE = Y, **2**; 5% Dy@**2**, **3**) were prepared by deprotonation of H_2L (*N*-(2-pyridylmethyl)-*N*,*N*-bis(2'-hydroxy-3',5'-di-*tert*-butylbenzyl)amine) with NaH, followed by reactions with anhydrous $RECl_3$ in THF (see ESI for details). Since they are isomorphous as confirmed by single-crystal X-ray diffraction, only the structure of complex **1** is discussed in detail (Table S1, ESI). Compound **1** crystallizes in space group *C*2/*c* and has a two-fold rotation axis passing through the two bridging chlorides (Figures 1 and S1, ESI). The Dy(III) ion has a seven-coordinate geometry completed by two phenoxide oxygen atoms and two nitrogen atoms from one tetra-chelated L^{2-}, two μ_2 bridging Cl^- and one THF molecule. The two $Dy–O_{(PhO)}$ bond lengths are 2.152(2) and 2.168(2) Å, much shorter than the $Dy–O_{THF}$ (2.412(2) Å), two Dy–N bonds (2.574(2) and 2.520(2) Å) and Dy–Cl bonds (2.7880(6) and 2.7896(6) Å) (Table S2, ESI). The local symmetry is not a regular polyhedron (as determined by Shape software,[10,11] see ESI Table S3), however the bond angle between the two short $Dy–O_{(PhO)}$ bonds = 149.62(8)° and this defines the main magnetic anisotropy axis as calculated by CASSCF-SO, giving an angle between the two main anisotropy axes of *ca.* 68° (see below). The Dy–Cl–Dy angles are 108.11(3) and 108.02(3)° and the Dy···Dy distance is 4.51 Å. The dinuclear motifs further stack via C–H···π interactions with the closest intermolecular Dy···Dy distance of 8.89 Å (Figure S2, ESI).

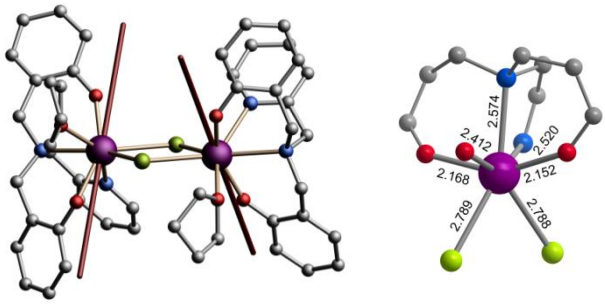

Figure 1. Molecular structure (left) and the coordination environment (right) of compound **1**. The red lines are the principal magnetic axes of the ground Kramers' doublets. Tert-butyl groups and H atoms are omitted for clarity. The unit of numbers is Å. Color codes: violet, Dy; green, Cl; blue, N; red, O and grey, C.

Temperature-dependent direct-current (dc) susceptibility data of **1** were collected under 1 kOe applied field. At room temperature the χT value is 28.53 $cm^3\ mol^{-1}\ K$, in good agreement with the expected value of 28.34 $cm^3\ mol^{-1}\ K$ for two Dy(III) ions (Figure S3, ESI). Upon cooling χT decreases slowly at first, and then more rapidly below 16 K, reaching 17.23 $cm^3\ mol^{-1}\ K$ at 2 K. The field-dependence of the magnetization reveals that the highest *M* value is 10.31 Nβ at 50 kOe and 2 K (Figure S4, ESI).

Alternating-current (ac) susceptibility measurements with an oscillating field of 3.5 Oe were also performed. Under zero dc field, **1** exhibits clear temperature and frequency dependence of the ac

[a] Dr. T. Han, Z.-H. Li, Dr. Y.-S. Ding, Prof. Y.-Z. Zheng
School of Science, Frontier Institute of Science and Technology (FIST), Research institute of Xi'an Jiaotong University (Zhejiang), State Key Laboratory for Mechanical Behavior of Materials, MOE Key Laboratory for Nonequilibrium Synthesis and Modulation of Condensed Matter, Xi'an Key Laboratory of Sustainable Energy and Materials Chemistry
Xi'an Jiaotong University
Xi'an 710049, China
E-mail: zheng.yanzhen@xjtu.edu.cn

[b] M. J. Giansiracusa, Dr. Y.-S. Ding, Dr. N. F. Chilton, Prof. Richard E. P. Winpenny
School of Chemistry
The University of Manchester
Oxford Road, Manchester M13 9PL, United Kingdom

Supporting information for this article includes synthetic procedures, structures, crystallographic details and additional figures.

susceptibility below 53 K, showing the typical slow magnetic relaxation of SMMs (Figures S5 and S6, ESI). The relaxation time (τ) at each temperature was extracted from a simultaneous fit of χ' and χ'' using the generalized Debye model.[12] The obtained parameters are summarized in Table S4, in which α values are always less than 0.07 in the temperature range of 8–53 K, indicating a narrow distribution of relaxation times (Figure S7, ESI). The α values found were converted into experimental uncertainties in the relaxation times for each temperature using the CC-FIT2 code.[12] We observe that relaxation on the timescale of our ac susceptibility experiments is dominated by a power-law temperature dependence characteristic of a two-phonon Raman process with $\log[C\ (s^{-1}\ K^{-n})] = -3.8 \pm 0.2$ and $n = 4.3 \pm 0.2$ (Figure 2, Equation 1).

At the highest temperatures there is an increase in the relaxation rate, likely indicative of a multi-phonon Orbach process with an exponential temperature dependence. Including the experimental uncertainties renders these parameters practically undefined with $U_{eff} = 1000 \pm 1000$ K and $\log[\tau_o\ (s)] = -10 \pm 10$. However, a U_{eff} value around 1000 K is independently supported by *ab initio* calculations, see below, and taking only the central relaxation rate, as has been the only approach in the literature prior to our new method,[12] a fit gives $U_{eff} = 922 \pm 9$ K, $\log[\tau_o\ (s)] = -11.33 \pm 0.08$ (Figure S8, ESI). The only higher U_{eff} value found for a polynuclear single-molecule magnets is in $Dy_2ScN@C80\text{-}I_h$.[13,14].

$$\frac{1}{\tau} = \frac{1}{\tau_0} e^{-U_{eff}/T} + CT^n \qquad (1)$$

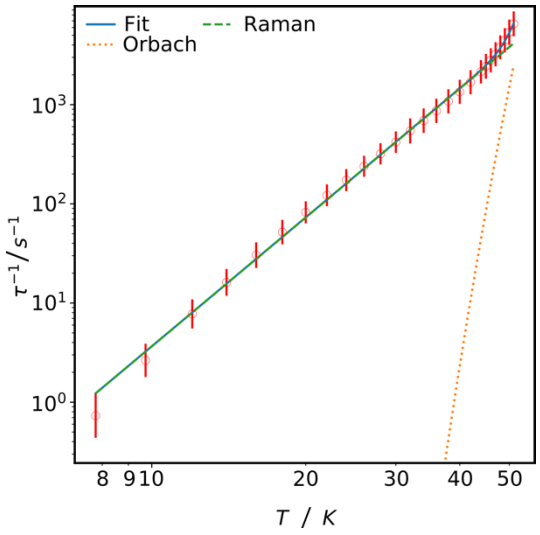

Figure 2. Plot of magnetic relaxation rate *vs.* temperature for **1**. Red circles are measured data with red bars which are uncertainties in magnetic relaxation times derived from generalized Debye fits. The solid blue line is the best fit by the *CC-FIT2* program,[12] the green dashed line is the Raman component and the orange dashed line is the Orbach component; as can clearly be seen the Orbach component is not defined by the experiment.

Field-cooled (FC) magnetization and zero-field-cooled (ZFC) magnetization for **1** show a divergence at 4.4 K which is also the maximum in the ZFC magnetization and hence we define the blocking temperature as 4.4 K (Figure S9, ESI).[1c] Magnetic hysteresis measurements on polycrystalline samples of **1** exhibit hysteresis loops open up to 6 K at an average sweep rate of 38 Oe s^{-1} (Figure S10, ESI). The coercive field (H_c) is 1250 Oe, and remnant magnetization (M_r) is 1.1 Nβ at 2 K. When the average sweep rate of hysteresis is lowered to 6 Oe/s, *S*-shaped curves are observed, and the H_c value decreases to 360 Oe at 0.5 K (Figures 3 and S11, ESI). The step at around 1018 Oe in the hysteresis loops up to 4 K is due to exchange-biasing of the magnetization which is usually observed at very low temperatures and on single crystals[8] or powder samples[8e] (Figures 3 and S12, ESI).

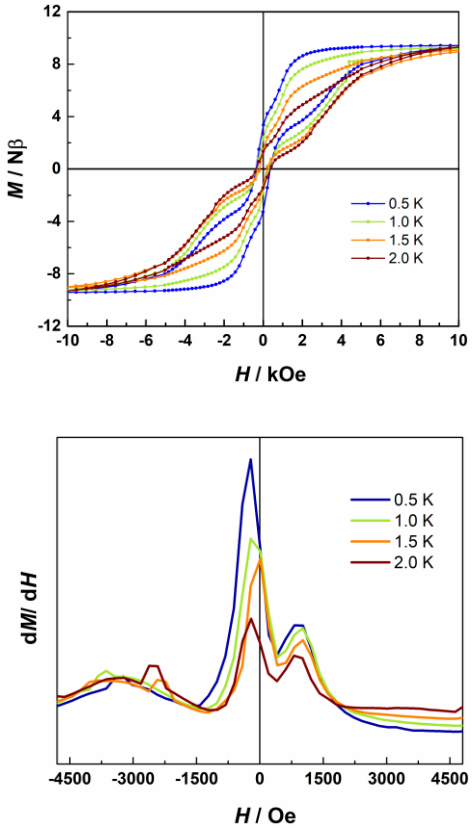

Figure 3. Plots of the magnetic hysteresis (top) and its first derivative (bottom) of a polycrystalline sample of **1** at an average sweep rate of 6 Oe/s. For clarity, the d*M*/d*H* data are obtained by averaging the positive to negative field sweep and the reversed negative to positive field sweep. The lines are guides for the eyes.

To examine the influence of the exchange-bias, we studied the magnetic properties of compound **3**, which contains a 5% concentration of Dy(III) ion doped into the isostructural diamagnetic yttrium dimer **2**. At this dilution level, the paramagnetic material is dominated by isolated Dy(III) ions in the structure.[8a] The dc magnetic susceptibility data and low temperature magnetisation data for **3** have very similar profiles to those of **1** (Figures S13–S15, ESI). Ac susceptibility measurements show slow relaxation of magnetization (Figures S16–S18, ESI), however the signal for **3** is much weaker owing to the dilution, and thus data can only be obtained up to 40 K and only Raman relaxation is observed in this temperature regime with $\log[C\ (s^{-1}\ K^{-n})] = -3.3 \pm 0.4$ and $n = 4.1 \pm 0.3$ (Figure S19, ESI). These parameters are statistically indistinguishable from those in **1**.

Cycling the field between +10 and –10 kOe for **3** gives a hysteresis loop shaped like a butterfly at low temperatures (Figures 4 and S20, ESI). The loss of magnetization at zero field for the diluted sample clearly confirms that magnetic interactions between Dy(III) ions in the dimer shifts the quantum tunnel resonances away from zero field. The two steps at ca. +1000 and –300 Oe for **1** are missing after dilution (Figures 3, 4, S12 and S21), and thus are markers of the magnetic interaction between the Dy(III) ions in the dimer.

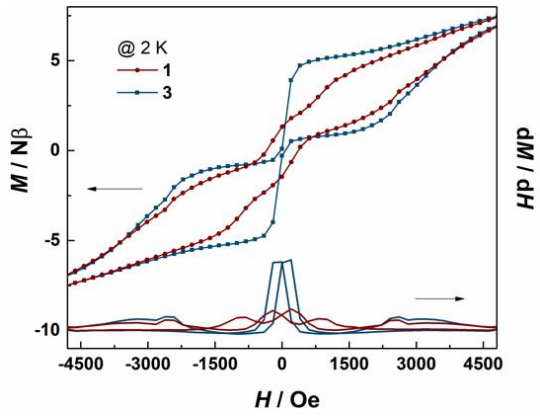

Figure 4. Hysteresis loop and its first derivative for **1** and **3** at 2 K at an average sweep rate of 6 Oe/s.

To understand the local electronic structure of the Dy(III) ions, complete active space self-consistent field spin-orbit (CASSCF-SO) calculations were performed using MOLCAS 8.0.[15a] Basis sets from the MOLCAS ANO-RCC library[15] were employed with the paramagnetic ion described using VTZP quality, the first coordination sphere with VDZP quality, and all other atoms with VDZ quality. To probe the single ion properties in the pure Dy compound **1**, one of the two Dy(III) ions in the crystal structure was replaced with the diamagnetic Lu(III) ion, as this more closely resembles the electronic manifold of the neighboring Dy(III) ion than would Y(III) (as Lu(III) has filled 4d, 5p and 4f orbitals). As expected based on the structure with a pair of phenoxide donors at an angle of 149.6°, the crystal field stabilizes an almost pure |±15/2⟩ ground doublet. This state is well separated from the 1st (534 K), 2nd (868 K) and 3rd (1053 K) excited states. While the 1st and 2nd excited states are fairly pure m_J = |±13/2⟩ and |±11/2⟩ functions respectively, the 3rd excited state is only 67% |±9/2⟩ (Table S5, ESI), and thus magnetic relaxation via the Orbach process is likely to occur through this state, predicting U_{eff} = 1053 K (Figure S22, ESI); this is in agreement with experimental value of 1000 K.

We can calculate the dipolar interaction between the two Dy(III) sites using the *g*-values and relative orientation of the *g*-frames from CASSCF-SO (Equation 2).[9,16] Owing to the two Dy(III) sites being related by a two-fold axis of rotation, the local anisotropy axes of the ions are not co-parallel, but rather the g_z axes have an angle of 68.25° between them. This gives the interaction matrix (Equation 3), which can be implemented in PHI to simulate the low temperature magnetic behavior (Equation 4).[17]

$$\overline{\overline{\mathrm{D}}}_{\mathrm{AB}} = \frac{{\mu_{\mathrm{B}}}^2}{\mathrm{r}^3}\left(\overline{\overline{\mathrm{g}}}_{\mathrm{A}} \cdot \overline{\overline{\mathrm{g}}}_{\mathrm{B}} \text{-} 3\left(\overline{\overline{\mathrm{g}}}_{\mathrm{A}} \cdot \vec{\mathrm{R}}\right) \cdot \left(\vec{\mathrm{R}}^{\mathrm{T}} \cdot \overline{\overline{\mathrm{g}}}_{\mathrm{B}}\right)\right) \quad (2)$$

$$\overline{\overline{D}}_{AB} = \begin{pmatrix} -0.23 & -0.16 & 0.03 \\ 0.16 & 0.11 & -0.02 \\ 0.03 & 0.02 & 0.00 \end{pmatrix} \quad (3)$$

$$\hat{H} = -2\hat{S}_A \cdot \overline{\overline{D}}_{AB} \cdot \hat{S}_B + \mu_B \vec{B} \cdot \left(\bar{\bar{g}}_A \cdot \hat{S}_A + \bar{\bar{g}}_B \cdot \hat{S}_B\right) \quad (4)$$

This purely dipolar interaction alone does not reproduce crossings or avoided crossings along any of the three main directions (Figures S23 and S24, ESI) corresponding to the steps in the hysteresis measurements, and instead predict a step only at zero field that is inconsistent with the experimental data. Therefore, there must be a non-zero superexchange interaction via the bridging chlorides. Compound **1** is EPR silent and therefore we were unable to directly measure the exchange interactions using EPR.[9,16]

For comparison, we could estimate the Ising exchange parameter considering the system as a simple Ising dimer, Equation (5), [8e,18] giving J_{Ising} = –1.88 cm^{-1} where H_{cross} is 1018 Oe from the first derivative of the magnetization, and *g* equals g_z = 19.87.

$$H_{\mathrm{cross}} = -J_{Ising}/2g\beta \quad (5)$$

Substituting J_{Ising} for J_{xx} in our simulations (because x in the molecular frame is the most magnetic direction, Figure S23) does not yield avoided crossings consistent with the QTM steps observed in the hysteresis measurements (Figure S25).[8d,19] Combining the dipole interaction matrix with the Ising approximation (*i.e.* Equation 3 with J_{xx} replaced with J_{Ising}) does predict an avoided crossing at *ca*. 1000 Oe, however, also predicts significant zero-field avoided crossing (contradicting experiment) and no evidence of the experimental feature at –300 Oe (Figure S26).

As none of these models fully explain the magnetization data, we have started with the dipole interaction matrix and added a superexchange component in order to reproduce the observed QTM steps. By addition +0.5 and –0.2 cm^{-1} to $J_{xx,}$ and J_{yy}, respectively, we find Zeeman simulations that predict avoided crossings consistent with the observed magnetization steps at *ca.* +1000 and –300 Oe (Figure 5). However, single crystal measurements at mK temperatures would be necessary to obtain accurate measurements of the low-lying magnetic states in **1** in order to verify the exchange model proposed here.

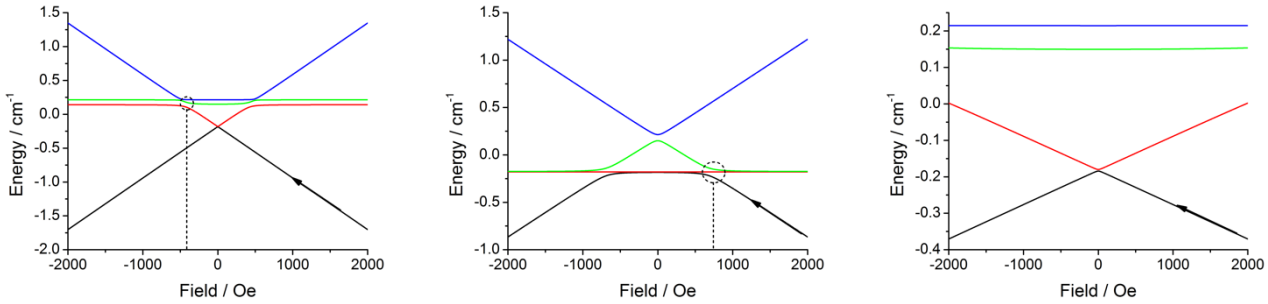

Figure 5 Simulation of the Zeeman diagram with $\overline{D}_{AB} = \begin{pmatrix} 0.27 & -0.16 & 0.03 \\ 0.16 & -0.09 & -0.02 \\ 0.03 & 0.02 & 0.00 \end{pmatrix}$. The magnetic field along the molecular *x*-axis (left), *y*-axis (centre) and *z*-axis (right). Note that there is a small avoided crossing at zero-field between the two ground states, with a gap of 4.27×10^{-3} cm^{-1}.

The parameters used to fit the relaxation behaviour of **1** and **3** can be compared with those found for other seven-coordinate Dy-SMMs with O-donors in the axial positions.[20] For example, in regular pentagonal bipyramids 900 < U_{eff} < 1300 cm^{-1}; log[τ_o (s)] = –11.63 ± 0.57; log[C (s^{-1} K^{-n})] = –6.03 ± 0.52; n = 4.1 ± 1.0. Thus, while U_{eff} and n are very similar both τ_o and C are bigger in the exchange-coupled dimer (log τ_o = –11.33 ± 0.08, log C = –3.41 ± 0.06). This may also be due to the less regular coordination environment in **1**. We have been able to switch off the zero-field loss of magnetisation in this high T SMM through exchange-biasing and this motivates us to improve the coupling strength while keeping the high anisotropy to construct better SMMs.

Experimental Section

Experimental Details can be found in the supplementary information.

Acknowledgements

This work was supported by NSFC (21871219 and 21773130), Key Laboratory Construction Program of Xi'an Municipal Bureau of Science and Technology (201805056ZD7CG40), the China Postdoctoral Science Foundation (2017M623150), the Shaanxi Postdoctoral Science Foundation (2017BSHTDZZ08), China Scholarship Council. NFC thanks The University of Manchester for a Presidential Fellowship and the Royal Society for a University Research Fellowship. MJG thanks The University of Manchester for a President's Doctoral Scholarship. REPW thanks the EPSRC for an Established Career Fellowship (EP/R011079/1) and the European Research Council for an Advanced Grant (ERC-2017-ADG-786734).

Keywords: Dinuclear Compound • Dysprosium • Exchange Interactions • Hysteresis Loop • Single-Molecule Magnet

[1] a) R. Sessoli, H.-L. Tsai, A. R. Schake, S. Wang, J. B. Vincent, K. Folting, D. Gatteschi, G. Christou, D. N. Hendrickson, *J. Am. Chem. Soc.* **1993**, *115*, 1804-1816. b) R. Sessoli, D. Gatteschi, A. Caneschi, M. A. Novak, *Nature* **1993**, *365*, 141-143. c) D. Gatteschi, R. Sessoli, J. Villain, *Molecular nanomagnets*, Oxford University Press, Oxford, **2006**.

[2] a) G. Christou, D. Gatteschi, D. N. Hendrickson, R. Sessoli, *MRS Bull.* **2000**, *25*, 66-71. b) M. N. Leuenberger, D. Loss, *Nature* **2001**, *410*, 789-793. c) L. Bogani, W. Wernsdorfer, *Nat. Mater.* **2008**, *7*, 179-186.

[3] a) C. A. P. Goodwin, F. Ortu, D. Reta, N. F. Chilton, D. P. Mills, *Nature* **2017**, *548*, 439-442. b) F.-S. Guo, B. M. Day, Y.-C. Chen, M.-L. Tong, A. Mansikkamäki, R. A. Layfield, *Science* **2018**, *362*, 1400-1403. c) K. R. McClain, C. A. Gould, K. Chakarawet, S. J. Teat, T. J. Groshens, J. R. Long, B. G. Harvey, *Chem. Sci.* **2018**, *9*, 8492-8503.

[4] a) J. Liu, Y. C. Chen, J. L. Liu, V. Vieru, L. Ungur, J. H. Jia, L. F. Chibotaru, Y. H. Lan, W. Wernsdorfer, S. Gao, X. M. Chen, M. L. Tong, *J. Am. Chem. Soc.* **2016**, *138*, 5441-5450. b) Y -S. Ding, N. F. Chilton, R. E. P. Winpenny, Y.-Z. Zheng, *Angew. Chem. Int. Edit.* **2016**, *55*, 16071-16074; *Angew. Chem.* **2016**, *128*, 16305-16308. c) Z. Jiang, L. Sun, Q. Yang, B. Yin, H. Ke, J. Han, Q. Wei, G. Xie, S. Chen, *J. Mater. Chem. C* **2018**, *6*, 4273-4280.

[5] a) K. X. Yu, Y. S. Ding, T. Han, J. D. Leng, Y. Z. Zheng, *Inorg. Chem. Front.* **2016**, *3*, 1028-1034. b) Y. S. Ding, T. Han, Y. Q. Hu, M. Xu, S. Yang, Y. Z. Zheng, *Inorg. Chem. Front.* **2016**, *3*, 798-807.

[6] a) D. N. Woodruff, R. E. P. Winpenny, R. A. Layfield, *Chem. Rev.* **2013**, *113*, 5110-5148. b) S. T. Liddle, J. van Slageren, *Chem. Soc. Rev.* **2015**, *44*, 6655-6669. c) J.-L. Liu, Y.-C. Chen, M.-L. Tong, *Chem. Soc. Rev.* **2018**, *47*, 2431-2453.

[7] W. Wernsdorfer, N. Aliaga-Alcalde, D. N. Hendrickson, G. Christou, *Nature* **2002**, *416*, 406-409.

[8] a) F. Habib, P.-H. Lin, J. Long, I. Korobkov, W. Wernsdorfer, M. Murugesu, *J. Am. Chem. Soc*. **2011**, *133*, 8830-8833. b) Y.-N. Guo, G.-F. Xu, W. Wernsdorfer, L. Ungur, Y. Guo, J. Tang, H.-J. Zhang, L. F. Chibotaru, A. K. Powell, *J. Am. Chem. Soc.* **2011**, *133*, 11948-11951. c) S. A. Sulway, R. A. Layfield, F. Tuna, W. Wernsdorfer, R. E. P. Winpenny, *Chem. Commun*. **2012**, *48*, 1508-1510; (d) E. M. Pineda, Y. Lan, O. Fuhr, W. Wernsdorfer, M. Ruben, *Chem. Sci.* **2017**, *8*, 1178-1185. e) J. Xiong, H. Y. Ding, Y. S. Meng, C. Gao, X. J. Zhang, Z. S. Meng, Y. Q. Zhang, W. Shi, B. W. Wang, S. Gao, *Chem. Sci.* **2017**, *8*, 1288-1294.

[9] E. Moreno-Pineda, N. F. Chilton, R. Marx, M. Dörfel, D. O. Sells, P. Neugebauer, S.-D. Jiang, D. Collison, J. van Slageren, E. J. L. McInnes, R. E. P. Winpenny, *Nat. Commun.* **2014**, *5*, 5243.

[10] a) H. Zabrodsky, S. Peleg, D. Avnir, *J. Am. Chem. Soc.* **1992**, *114*, 7843-7851. b) M. Pinsky, D. Avnir, *Inorg. Chem.* **1998**, *37*, 5575-5582.

[11] P. Llunell, M. Casanova, D. Cirera, J. Bofill, J. M. Alemany, D. Alvarez, S. Pinsky, M. Avnir, *SHAPE 2.1*, Universitat de Barcelona and The Hebrew University of Jerusalem, Barcelona and Jerusalem, **2003**.

[12] a) D. Reta and N. F. Chilton, *ChemRxiv*, **2019**, doi: 10.26434/chemrxiv.8863904.v1. b) CC-FIT2 is available from http://www.nfchilton.com/cc-fit.

[13] D. S. Krylov, F. Liu, S. M. Avdoshenko, L. Spree, B. Weise, A. Waske, A. U. B. Wolter, B. Büchner, A. A. Popov, *Chem. Commun*. **2017**, *53*, 7901-7904.

[14] a) R. J. Blagg, L. Ungur, F. Tuna, J. Speak, P. Comar, D. Collison, W. Wernsdorfer, E. J. L. McInnes, L. F. Chibotaru, R. E. P. Winpenny, *Nature Chem.* **2013**, ***5***, 673-678. b) R. J. Blagg, C. A. Muryn, E. J. L. McInnes, F. Tuna, R. E. P. Winpenny, *Angew. Chem. Int. Edit.* **2011**, *50*, 6530-6533; *Angew. Chem.* **2011**, *123*, 6660-6663. c) T. Han, Y.-S. Ding, Z.-H. Li, K.-X. Yu, Y.-Q. Zhai, N. F. Chilton and Y.-Z. Zheng, *Chem. Commun*. **2019**, *55*, 7930-7933. d) S. Demir, M. I. Gonzalez, L. E. Darago, W. J. Evans, J. R. Long, *Nature Commun.* **2017**, *8*, 2144.

[15] a) F. Aquilante, J. Autschbach, R. K. Carlson, L. F. Chibotaru, M. G. Delcey, L. De Vico, I. Fdez. Galván, N. Ferré, L. M. Frutos, L. Gagliardi, M. Garavelli, A. Giussani, C. E. Hoyer, G. Li Manni, H. Lischka, D. Ma, P. Å. Malmqvist, T. Müller, A. Nenov, M. Olivucci, T. B. Pedersen, D. Peng, F. Plasser, B. Pritchard, M. Reiher, I. Rivalta, I. Schapiro, J. Segarra-Martí, M. Stenrup, D. G. Truhlar, L. Ungur, A. Valentini, S. Vancoillie, V. Veryazov, V. P. Vysotskiy, O. Weingart, F. Zapata, R. *J.* Lindh, *Comput. Chem.* **2016**, *37*, 506-541. b) B. O. Roos, R. Lindh, P.-Å. Malmqvist, V. Veryazov, P.-O. Widmark, *J. Phys. Chem. A* **2008**, *112*, 11431-11435. c) B. O. Roos, R. Lindh, P. Å. Malmqvist, V. Veryazov, P. O. Widmark, *J. Phys. Chem. A* **2004**, *108*, 2851-2858.

[16] M. J. Giansiracusa, E. Moreno-Pineda, R. Hussain, R. Marx, M. Martínez Prada, P. Neugebauer, S. Al-Badran, D. Collison, F. Tuna, J. Van Slageren, S. Carretta, T. Guidi, E. J. L. McInnes, R. E. P. Winpenny, N. F. Chilton, *J. Am. Chem. Soc.* **2018**, *140*, 2504-2513.

[17] N. F. Chilton, R. P. Anderson, L. D. Turner, A. Soncini, K. S. Murray, *J. Comput. Chem.* **2013**, *34*, 1164-1175.

[18] a) F. Pointillart, Y. L. Gal, S. Golhen, O Cador, L. Ouahab, *Chem. Eur. J.* **2011**, *17*, 10397-10404. b) X. Yi, K. Bernot, F. Pointillart, G. Poneti, G. Calvez, C. Daiguebonne, O. Guillou, R. Sessoli, *Chem. Eur. J.* **2012**, *18*, 11379-11387.

[19] E. Moreno-Pineda, M. Damjanović, O. Fuhr, W. Wernsdorfer, M. Ruben, *Angew. Chem. Int. Edit.* **2017**, *56*, 9915-9919; *Angew. Chem.* **2017**, *129*, 10047-10051.

[20] Y.-S. Ding, T. Han, Y.-Q. Zhai, D. Reta, N. F. Chilton, Y.-Z. Zheng, R. E. P. Winpenny, submitted.

Table of Contents